Civil Engineering Dimension, Vol. 25, No. 1, March 2023, 20-28
ISSN 1410-9530 print / ISSN 1979-570X online
DOI: https://doi.org/10.9744/CED.25.1.20-28

Application of Soil Structure Interaction on Building with Basement using Nonlinear Soil Springs

Jesica, A.[1], Pudjisuryadi, P.[2*], and Rosidi, D.[3]

Abstract: In a typical building design, the interaction between building and surrounding soils is often ignored. Since soil is deformable and has limited capacity to resist loads, this interaction, called soil-structure interaction (SSI), could alter building responses, especially during earthquake loadings for buildings with significant basement depths. In this study, a 10-story reinforced concrete building with 3-level basement was used to evaluate the effects of SSI on building during earthquakes. Dynamic time response analyses were performed using earthquake time histories scaled to a design response spectrum for a Surabaya, Indonesia, location. Soil responses during earthquakes were modeled using nonlinear hysteresis normal and elastic-perfectly plastic frictional soil springs, developed using the hardening soil with small strain stiffness model. Depth-varying ground motions were also applied along the basement depth. The results show inconclusive SSI effects, where some of the time histories produce greater base shears and inter-story drifts when SSI is considered, while others show the opposite results.

Keywords: Soil structure interaction; nonlinear soil spring; building with basement; dynamic time response analysis; base shear; inter-story drift.

Introduction

In an urban setting, where land is limited, higher buildings with significant basement depth are often built to maximize the land use. Design of these structures typically assumes a fixed base or a hinge base, an assumption that could be very different from the reality. Soils supporting the structure can deform vertically and horizontally (i.e., not a fixed base), and hence, may impact structural behavior, especially during earthquakes. The interaction between structure and soil is commonly called soil structure interaction (SSI). SSI considerations result in a longer structural fundamental period and may increase or decrease the base shear, depending on the structural flexibility, as shown in Figure 1 [1]. A lower base shear means lower internal forces on the structural elements, which translate to lower construction costs.

Past studies have shown the significant effects of SSI on structural responses during earthquakes [2-6].

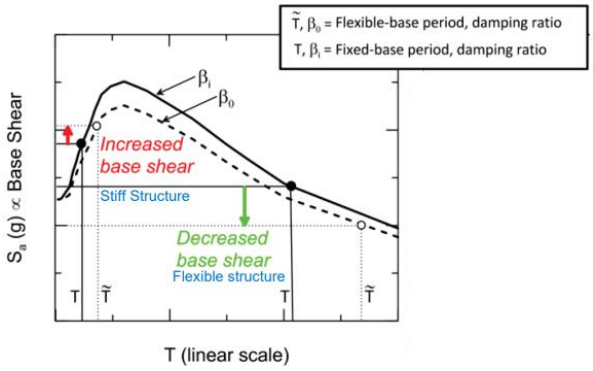

Figure 1. SSI Effects on Structural Base Shear [1]

In general, these studies adopted the following two approaches to analyze the effects of SSI on a structure: (1) the direct method, where soils and structure are modeled together, and (2) the indirect method, where soil behaviors are represented using springs. For example, Dabhi et al. [2] evaluated several multi-story buildings with basements using the indirect method and linear soil springs obtained using the procedures as outlined in the FEMA 356 publication [7]. The results indicated longer structural fundamental periods (as expected) and significant reduction in structural base shear and moment when SSI is considered. Other study by Khoueiry and Khouri [3] analyzed multi-story structures with up to 7 basement levels. In Khoueiry and Khouri's study [3], the direct and indirect analysis methods with and without SSI were both considered for structures on hard, dense, and soft soils. The soil model used was the simple linear-elastic-perfectly-plastic Mohr-

[1] Structural Engineer, Benjamin Gideon and Associates Consulting Engineers, Surabaya, INDONESIA
[2] Department of Civil Engineering and Planning Petra Christian University, Surabaya, INDONESIA
[3] Sr. Principal Geotechnical Engineer, Jacobs Engineering Group, Oakland, California, USA
*Corresponding author; Email: pamuda@petra.ac.id

Note: Discussion is expected before July, 1st 2023, and will be published in the "Civil Engineering Dimension", volume 25, number 2, September 2023.

Received 02 March 2023; revised 15 March 2023; accepted 16 March 2023.

Coulomb model. Two observations can be made from this study: 1) importance of SSI for tall buildings, especially for buildings on soft soils (soil class E) and 2) the structural top displacement and natural frequency computed using the direct method are similar to those obtained using the indirect method with proper considerations of SSI.

This current study evaluated a 10-story reinforced concrete building with 3-level basement. The indirect method was used, where soil responses or springs against the basement wall movements during earthquakes were developed using the finite element computer program PLAXIS [8] by considering the nonlinear hysteresis hardening soil with small strain stiffness soil model. This soil model can reasonably capture the nonlinearity and hysteretic behaviors of soil. Both the normal and frictional soil springs were developed for the basement walls and bottom slab. In addition, depth-varying ground motions were applied along the basement walls to account for the variation of ground motions with depth. Dynamic time response analyses were performed using 5 (five) earthquake time histories recorded during past earthquakes. These time histories were scaled to a stiff soil design response spectrum for a location in Surabaya, Indonesia, and propagated upward to the ground surface. Seismic performances in terms of building inter-story drift and base shear were used to assess the effects of SSI.

Development of Soil Springs

As stated before, soil springs for the analysis were developed using the computer program PLAXIS [8] by considering the nonlinear hysteresis Hardening Soil with Small Strain Stiffness soil model. The soil model parameters were calibrated using the available soil data obtained from soil borings drilled at the location considered in this study [9].

Soil Data and Soil Parameter Calibration

The available soil boring data indicate the subsurface soils consist mostly of clayey soils, underlying ±4.5 meters of clayey fine sands. Table 1 summarizes the idealized soil profile and engineering parameters obtained from the soil borings, laboratory testing results and correlations with SPT N-values. Groundwater was taken at 1 (one) meter below the ground surface. The undrained shear strength, S_u, and the small-strain shear wave velocity, V_s, were estimated using the following published correlations with SPT N-values:

$$S_u = P_a \times 0.29\, N_{60}^{0.72} \text{ [10]} \quad (1)$$

Where P_a is atmosphere pressure ($101.325\, {}^{kN}/_{m^2}$), and N_{60} is SPT N-values normalized to a 60% hammer energy efficiency.

$$V_s = \exp[\,\beta_0 + \beta 1\, \ln(N_{60}) + \beta_2 \ln(\sigma_v')] \quad \text{[11]} \quad (2)$$

where σ_v' is effective vertical stress and β is the regression parameter shown at Table 1.

Table 1. Idealized Soil Profile and Engineering Parameters

Layer	depth (m)	N_{60} (blows/30cm)	γ_{sat} (kN/m³)	ϕ (deg)	S_u (kN/m²)
Layer 0 - Compacted Fill	0	75	20.42	38	0
	1.5	75			
Layer 1 - Clayey Fine Sand	1.5	2	16.23	38	0
	3	3			
	4.5	3			
	6	2			
Layer 2 - Grey Clay	6	2	17.49	0	48
	7.5	3			65
	9	4			80
Layer 3 - Grey Clay	9	4	17.49	0	80
	10.5	9			143
Layer 4 - Silty Grey Clay	10.5	9	17.49	0	143
	12	11			165
	13.5	12			176
	15	14			196
Layer 5 - Dark Brown Grey Clay	15	14	17.49	0	196
	16.5	16			216
	18	20			254
	19.5	13			186
	21	17			226
Layer 6 - Silty Brown Clay	21	17	17.49	0	226
	22.5	17			226
	24	20			254
	25.5	16			216
	27	19			245
	28.5	16			216
	30	19			245

The maximum shear modulus, G_{max}, was then obtained from Vs, as follow:

$$G_{max} = V_s^2 \times \rho = V_s^2 \times \gamma_t / g \quad (3)$$

where g is gravity acceleration and γ_t is total unit weight.

The estimated S_u, and V_s values with depth are listed in Table 2 and plotted on Figure 2 (solid blue line), respectively.

Table 2. Regression Parameter

Soil type	β_0	β_1	β_2
Sand	4.045	0.096	0.236
Silt	3.783	0.178	0.231
Clay	3.996	0.230	0.164

The Hardening Soil with Small Strain Stiffness soil model in PLAXIS [8] is a nonlinear soil model capable of simulating cyclic soil responses during earthquakes (i.e., initial loading, unloading and reloading). The model has adopted a stress-dependent shear modulus:

$$G_{max} = G_{max}^{ref} \left[\frac{c \times cos\emptyset - \sigma_3' \times sin\emptyset}{c \times cos\emptyset + p^{ref} \times sin\emptyset} \right]^m \quad (4)$$

The reference stress, p^{ref}, was taken as 100 kN/m^2 and m was set to 0.5 for sandy soils and 1 for clayey soils. The calibration of the soil model was carried out by adjusting the reference shear modulus, G_{max}^{ref} for each soil layer untill the G_{max} values matched reasonably well with those estimated from the soil data. Figure 2 compares the V_s values (derived from G_{max} through Eq. 3 above) estimated from the soil model and soil data (SPT N-values). As can be seen from Figure 2, the V_s values predicted by the soil model match well to those obtained from the soil data.

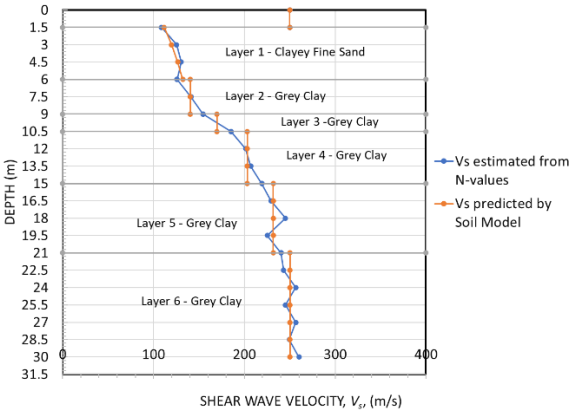

Figure 2. Comparison of Small-strain V_s Profile obtained from Soil Data and Soil Model

Soil Springs

To develop the nonlinear hysteresis soil normal springs, the finite element computer program PLAXIS [8] and the calibrated Hardening Soil model were used. The soil normal springs were developed by pushing the basement wall back and forth (i.e., by applying a cyclic wall displacement against the soils) and recording the corresponding soil pressures at the wall-soil interface. The soil normal spring, as a function of wall movement or deflection, was then defined as the ratio of soil pressure or force over a unit of wall deflection. The estimated relations between wall movement and force are plotted in Figures 3 and 4 for the bottom slab and at select depths along the basement wall, respectively. These figures clearly show the nonlinear and hysteresis behavior of soil springs. It should be noted that the calculated soil responses for depths less than ±5 meters are not well-behaved; likely due to the low stiffness (V_s of about 120 m/s) of the clayey fine sands. For the frictional spring, a linear perfectly plastic load-deflection curve was used, obtained by multiplying a frictional coefficient to the normal force, as depicted on Figure 5.

For the structural dynamic analysis, the soil springs are represented by the Link Elements in the structural program SAP2000 V.21 [12]. These Link Elements are then connected to nodes that represent soils, where seismic ground displacements are prescribed. Therefore, these Link Elements need to be calibrated, so their responses are similar to those observed in the PLAXIS model. Links were installed at 1.5 m and 6 m spacings along the basement walls and basement slab, respectively. These spacings were selected by considering the soil layer thicknesses along the walls and the column spans. Figure 3 and 4 depicts the force-displacement relations calculated using the Link Elements in SAP2000 [12], illustrating reasonable matches in force-displacement relations predicted by the PLAXIS [8] and SAP2000 models [12], except for link on basement wall with depths less than ±5 meters.

Depth-Varying Ground Motions

The depth-varying earthquake ground motions along the basement wall were calculated using the one-dimensional (1D) site response analysis.

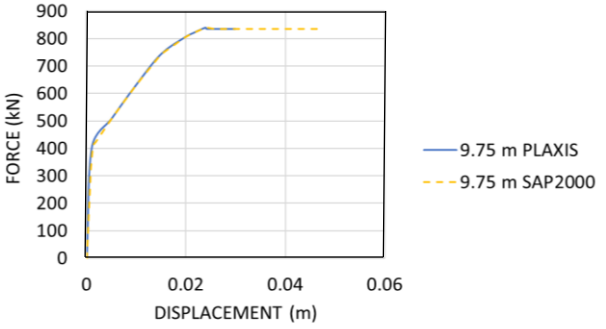

Figure 3. Load-deflection Curve for Soil Normal Spring Calculated for Basement Bottom Slab

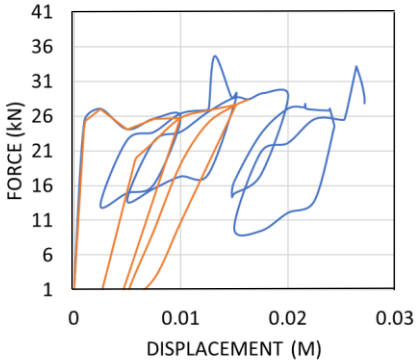

(a) depth=0.75 m

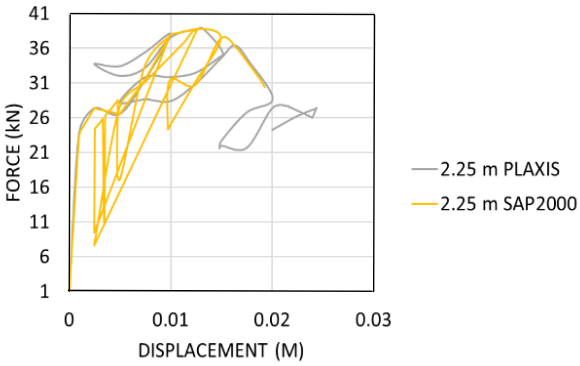

(b) depth = 2.25 m

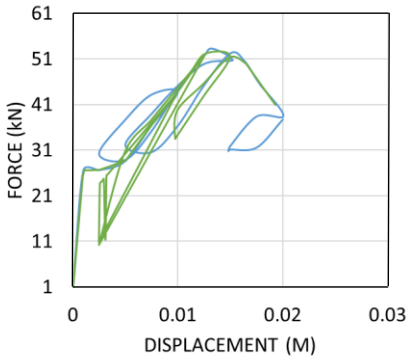

(c) depth = 3.75 m

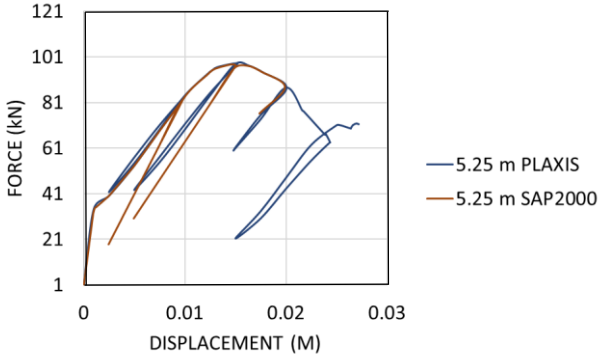

(d) depth = 5.25 m

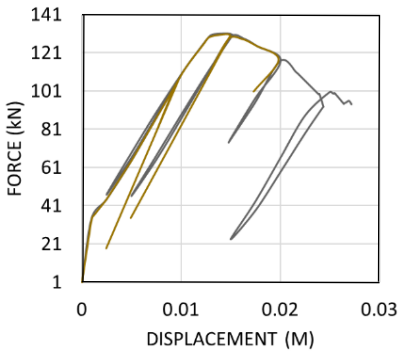

(e) depth = 6.75 m

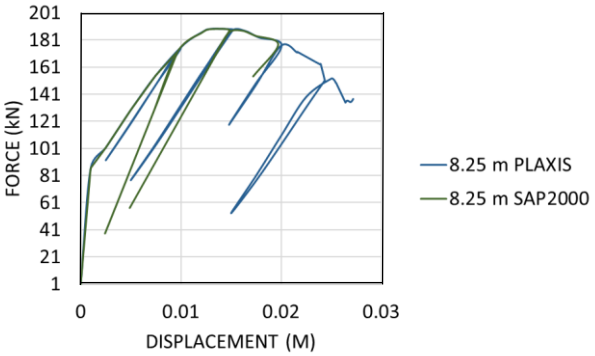

(f) depth = 8.25 m

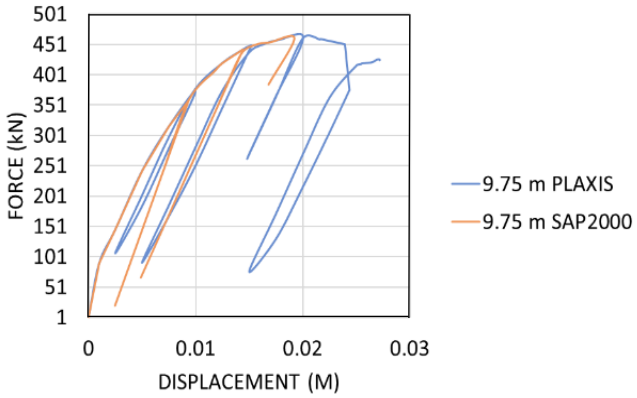

(g) depth = 9.75 m

Figure 4. Load-deflection Curves for Soil Normal Springs Calculated at Select Depths Along Basement Wall

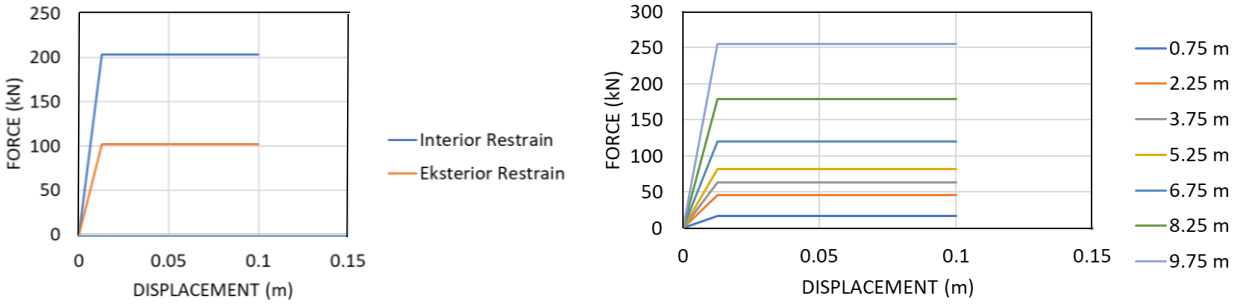

(a) Base slab (b) Basement wall

Figure 5. Load-deflection Curves for Soil Frictional Springs Calculated at Select Depths along Basement Wall and Base Slab

Table 3. Earthquake Time Histories used for the Site Response Analysis [15]

Earthquake	Year	Station	Magnitude	Mechanism	R_{rup} (km)	V_{s30} (m/sec)
Northridge-01	1994	Alhambra - Fremont School	6.69	Reverse	37	550
Imperial Valley-02	1940	El Centro Array9	6.95	strike slip	6	213
Kobe_ Japan	1995	Takatori	6.9	strike slip	1.5	256
Kocaeli_ Turkey	1999	Tekirdag	7.51	strike slip	165	522
Chi-Chi_ Taiwan	1999	CHY002	7.62	Reverse Oblique	25	235

Notes: R_{rup} = rupture distance; V_{s30} = time-averaged V_s in the top 30 m.

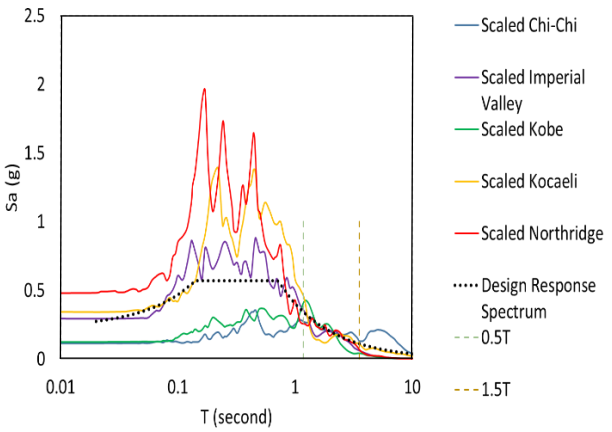

Figure 6. Comparison of Target and Scaled Time History Response Spectra

Table 3 lists the 5 (five) time histories recorded during past earthquakes and used for the analysis. The selection of these time histories was based on the fault mechanisms that control the seismic hazards in Surabaya, as well as the controlling magnitudes and distances [13]. These selected time histories were first scaled, so that their average response spectral values in the period range of interest (0.5 T to 1.5 T, where T is the structural fundamental period) matched well to those of a target spectrum for a location in Surabaya and a soil site class D (stiff soil site). Figure 6 compares the target design spectrum and the response spectra calculated from the scaled time histories.

These scaled time histories were then inputted at a depth of 60 meters on a stiff soil and propagated upward in the site response analysis to obtain the depth-varying earthquake ground displacement time histories along the basement wall. The site response analysis was conducted using the computer program Deepsoil V.7. [14], and the calculated ground displacement time histories at select depths along the basement wall are plotted in Figure 7 for the 1999 Chi-Chi earthquake record. Similar displacement time histories were also obtained for the other earthquake records.

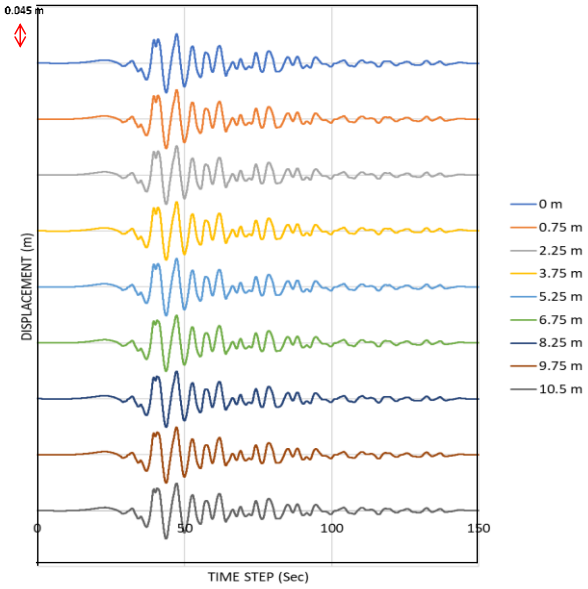

Figure 7. Calculated Ground Displacement Time Histories at Select Depths along Basement Wall for the 1999 Chi-Chi Earthquake

Structural Dynamic Time Response Analysis

As stated previously, the building analyzed for this study is a typical 10-story reinforced concrete office structure with basement in Surabaya, Indonesia, founded on stiff soils (soil site class D). The building floor plan and height were chosen based on a simple check for SSI considerations that includes embedment depth, upper structure height and natural period, and average shear wave velocity [16]. In this check, when the structure effective height devided by shear wave velocity (V_s) and building period (T) is greater than 0.1, SSI should be considered.

Structural Dimension and Data

Figure 8 depicts the selected building floor plan and structural data. The column and beam dimensions were determined based on the anticipated dead and live loads for an office building [17].

Table 4 and Figure 9 describe the four (4) types of building-foundation soil connection analyzed for this study to evaluate the effects of SSI on building seismic responses. The fourth model (nonSSI-2) is the simplest structural model, and it is the most commonly used in practices. Also listed on Table 4 are the fundamental periods calculated for these structural models. The periods are quite similar, with that calculated for structure with SSI being slightly longer. This is due to the use of the initial (maximimum) soil spring stiffness in calculating these fundamental periods. However, during earthquake shaking and as the soil spring degrades, the period of structure with SSI will gradually become longer.

Structural Seismic Performances

Dynamic structural time response analyses were conducted to evaluate the effects of SSI on building seismic performances. The effects of SSI were assessed in terms of inter-story drift and structural

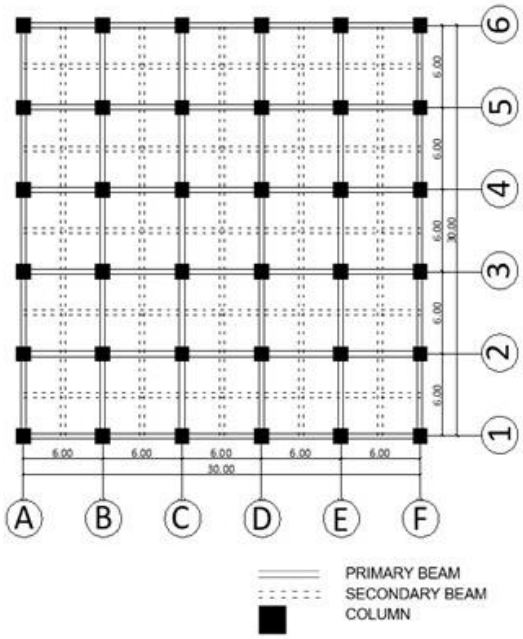

Parameter	
Total floors	10 floors + 3 level of basement
Building's area	30 m x 30 m
Column to column span	6 m
Total building height	3.5 m x 10 floors= 35 m
Basement Depth	3.5 m x 3 floors = 10.5 m
Slab thickness	120 mm
Concrete strength	fc' 30 MPa

Level	Structure Element	Label	Width [mm]	Depth [mm]
Basement 3 - 1	Column	K1	800	800
2-5	Column	K2	700	700
6	Column	K3	600	600
7	Column	K4	500	500
8-9	Column	K5	400	400
10	Column	K6	300	300
Basement 2- 10	Primary Beam	BI	250	500
Basement 2-10	Secondary Beam	BA	200	400
Basement 2-10	Floor Slab	PL	-	120
Basement 3	Base Slab	PD	-	1000
Basement 3- Basement 2	Wall	PD	-	1000

Figure 8. Seleted Building Floor Plan and Structural Data

Table 4. Building-foundation Soil Connections Analyzed for This Study

Case ID	Case Descriptions	Initial Fundamental Period (seconds)
SSI-1	Considers SSI (soil springs) and depth-varying ground motions	2.03
SSI-2	Considers SSI (soil springs) and uniform ground motions	2.03
NonSSI-1	Considers fixed connections along basement walls and uniform ground motions	1.95
NonSSI-2	Considers fixed connections at top of basement and uniform ground motions	1.91

Notes: For the cases with uniform ground motions, the ground motions calculated at the top of basement were used.

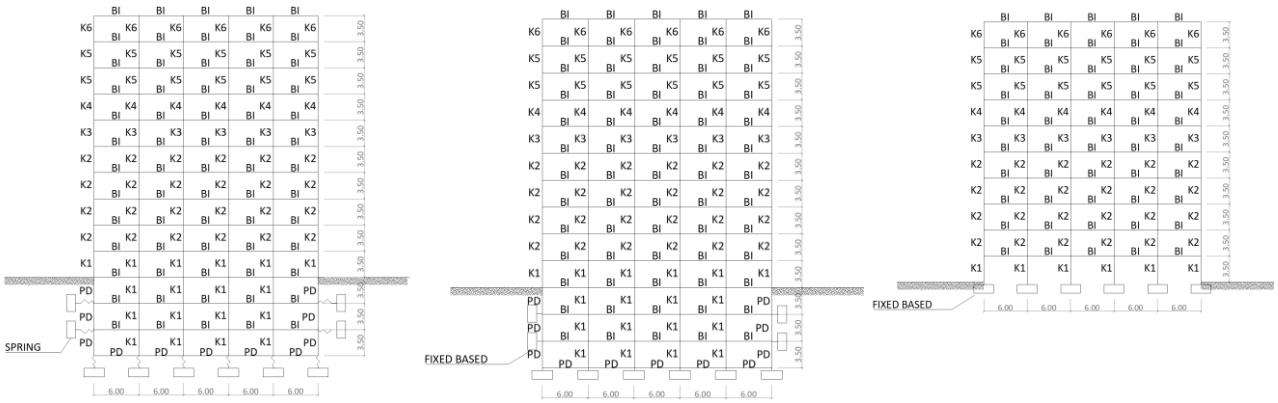

SSI-1 and SSI-2 NonSSI-1 NonSSI-2

Figure 9. Building-foundation soil Connections Analyzed for This Study

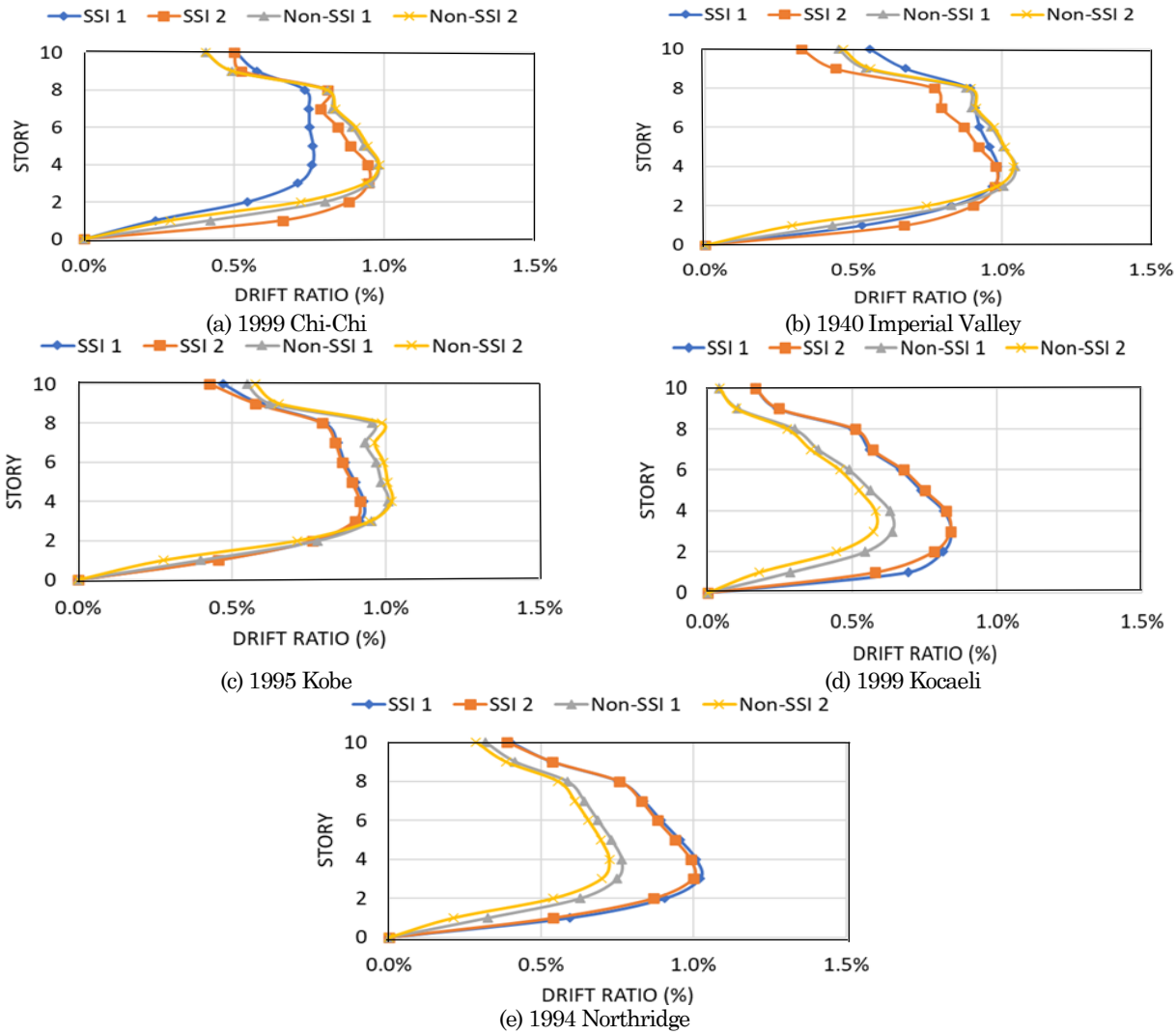

(a) 1999 Chi-Chi (b) 1940 Imperial Valley

(c) 1995 Kobe (d) 1999 Kocaeli

(e) 1994 Northridge

Figure 10. Calculated Inter-story Drifts

base shear. The structural elements (i.e., beams, columns, slabs and walls) were modeled as linear elastic elements, with no hinges or plastic deformations allowed to develop during shaking. In reality, plastic hinges will likely develop in columns and/or beams during strong ground shakings, which in turn, will absorpt the earthquake energy due to material ductility and will reduce the element forces. Based on SNI 1726:2019 [18], to account for this reduction in forces due to ductility in reinforced concrete, the input ground motions for the structural analyes were reduced by a factor of 8 (an R-factor of 8).

Inter-Story Drifts

Figure 10 shows the building inter-story drifts calculated for the 4 (four) structural models and 5 (five) earthquake time histories. The building inter-story drifts were taken at the time-step when the largest drift ratio occured. Furthermore, to account for the anticipated building inelastic behavior, the calculated drifts were multiplied by a deflection magnification factor, *Cd,* of 5.5 and divided by the seismic importance factor, *Ie,* of 1.0 [18]. The results indicate the following:

1. When SSI is considered, 3 (three) of the time histories (the 1999 Chi-Chi, 1940 Imperial Valley and 1995 Kobe earthquakes) predict smaller inter-story dirfts, while the other 2 (two) records (the 1999 Kocaeli and 1994 Northridge earthquakes) result in larger drifts.
2. The use of depth-varying ground motions along the basement wall has insignificant effects on drifts, except for the 1999 Chi-Chi earthquake and to a lesser degree for the 1940 Imperial Valley earthquake.
3. The calculated drifts are very similar for the two non-SSI models (NonSSI-1 and NonSSI-2), as expected, since the building is effectively fixed at the top of basement.
4. The maximum drifts occur on floor level 3 or 4 and all calculated drifts are less than 1.1%, which is below the design limit of 2% for risk category I structures set by the SNI 1726: 2019 [18].

Structure Base Shear

The structure base shear was taken by first summing all the base shears in the columns at each earthquake loading increment, and then taking the absolute maximum value. Figure 11 and Table 5 summarize the structural base shears calculated for the 4 (four) analysis models and 5 (five) earthquake time histories.

As for the inter-story drift, similar results are observed for the structural base shear:

1. When SSI is considered, 3 (three) of the time histories (the 1999 Chi-Chi, 1940 Imperial Valley and 1995 Kobe earthquakes) predict smaller base shears, while the other two records (the 1999 Kocaeli and 1994 Northridge earthquakes) result in larger base shears.
2. A reduction of about 40% in base shear is observed for the 1999 Chi-Chi earthquake when SSI and depth-varying ground motions are considered (±235 KN versus ±380 KN; see Table 5).
3. The use of depth-varying ground motions along the basement wall has insignificant effects on base shears, except for the 1999 Chi-Chi earthquake.
4. The calculated base shears are similar for the two non-SSI models (NonSSI-1 and NonSSI-2), as expected.

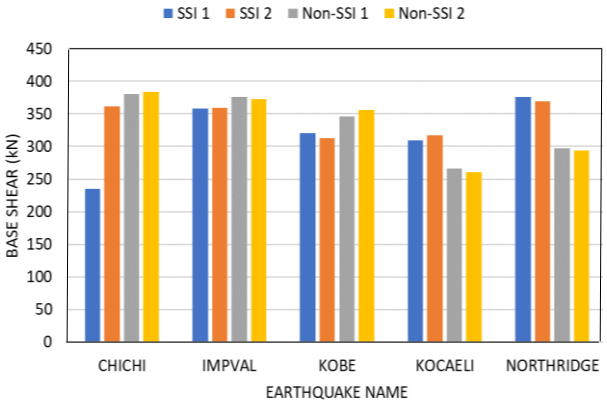

Figure 11. Calculated Base Shears

Looking at Figure 6, 2 (two) of the earthquake time histories that result in smaller drifts and base shears are those below the target spectrum for periods less than ±1 second (outside the range of spectral scaling), while the other two that produce larger drifts and base shears are those scaled above the target for periods less than 1 second. These results may suggest that current practice of scaling the time history only within a limited period range of interest around building fundamental period may lead to inconsistent results and highlight the importance of selecting records with similar spectral shape.

Conclusion

This study attempts to evaluate the effects of SSI on a typical reinforced concrete office building in Surabaya, Indonesia. The SSI was modeled using soil

Table 5. Calculated Base Shears

Type → / Earthquake Name↓	SSI-1		SSI-2		NonSSI-1		NonSSI-2	
	Base Shear (kN)	Time Step (sec)	Base Shear (kN)	Time Step (sec)	Base Shear (kN)	Time Step (sec)	Base Shear (kN)	Time Step (sec)
1999 Chi-Chi	234.59	40.88	361.78	42.00	380.69	41.84	383.88	41.81
1940 Imp. Valley	358.48	20.93	358.97	20.96	376.12	20.81	372.55	20.77
1995 Kobe	320.09	23.84	313.00	22.80	346.30	24.61	355.66	25.50
1999 Kocaeli	309.14	39.51	317.61	39.44	266.63	39.37	261.12	39.35
1994 Northridge	376.44	42.92	369.84	41.82	296.76	41.70	294.09	41.68

*Time Step= the time when absolute maximum total base shear happened

springs and the indirect analysis method, where the structure and soils were modeled separately. To simulate the nonlinear soil spring behavior, the finite element computer program PLAXIS [8] and the nonlinear hysteresis Hardening Soil with Small Strain Stiffness soil model were used. The nonlinear soil model was calibrated using the soil data collected for a site in Surabaya.

Structural dynamic time response analyses were performed using earthquake time histories recorded during past earthquakes to assess the building seismic performances, in terms of inter-story drift and base shear. The results show some of the time histories predict larger base shears and maximum inter-story drifts when SSI is considered, while others show the opposite results. These results indicate that the effects of SSI on building seismic performances could be insignificant or inconclusive in some cases. For this study, this may be due to the fact that the design earthquake ground motions are relatively low (after a R-value of 8 is applied), the basement is stiff, and the soil underneath the basement is dense, resulting in small rotation and/or racking of the basement, and hence, insignificant SSI between the basement and the surrounding soils. The selection of earthquake time histories is also found to be an important factor.

For future studies, it is recommended that improvements could be made to better assess the effects of SSI on building seismic performances, including use of nonlinear structural elements and softer foundation soils and assessments of SSI effects as a function of relative stiffness between basement and surrounding soils.

References

1. NIST GCR 12-917-21, *Soil-Structure Interaction for Building Structures*, NEHRP Consultants Joint Venture, 2008 .
2. Dabhi G., Agrawal, V.V., and Patel, V.B., Soil Structure Interaction for Basement System of Multi Storey Building for Different Soil Condition using Static Analysis in Etabs, *SSRG International Journal of Civil Engineering*, 7(6), 2020, pp. 71-79.
3. Khoueiry, D.H. and Khouri, M.F, Integrating *Soil-Structure Interaction* along *Basement* Walls in Structural *Analysis* Programs, *International Journal of Development and Research*, 5(04), 2015, pp. 4061-4068.
4. Chen, J.C., Rosidi, D., and Lee, L., Soil-Structure Interaction for Seismic Analysis of A Nuclear Facility, *Proceedings of the 9th U.S. Nasional and 10th Canadian Conference on Earthquake Engineering*, Toronto, Canada, July 25-29, 2020, pp.717-724.
5. Hu, J.J. and Xie, L.L., Variation of Earthquake Ground Motion with Depth, *ACTA SEISMOLGICA SINICA*, 18(1), 2004, pp. 72-81
6. Mercado, J.A., Arboleda-Monsalve, and Terzic, V., Seismic Soil-Structure Interaction Response of Tall Building, *Geo-Congress 2019: Earthquake Engineering and Soil Dynamics GSP,* 308(1), ASCE, 2019, pp.118-128.
7. FEMA 356, *Prestandard and Commentary for The Seismic Rehabilitation of Builldings,* American Society of Civil Engineers Virginia, 2000.
8. *PLAXIS Version 8.6*, Bentley, 2011.
9. Setyobudi, G., Hasil Penyelidikan Tanah Gedung P1 dan P2 UK Petra Surabaya, Laboratorium Mekanika Tanah Universitas Kristen Petra, Surabaya, 2011.
10. Hara, A., Ohta, T., Niwa, M., Tanaka, S., and Banno, T., Shear Modulus and Shear Strength of Cohesive Soils, *Soils and Foundation*, 14(3), 1974, pp. 1-12.
11. Brandenberg, S.J., Bellana, N., and Shantz, T., Shear Wave Velocity as Function of Standard Penetration Test Resistance and Vertical Effective Stress at California Bridge Sites, *Soil Dynamics and Earthquake Engineering,* 30(2010), 2010, 1026-1035.
12. SAP2000 Integrated Software for Structural Analysis and Design Version 21, Computer and Structures, Inc, 2018.
13. *Peta Deagregasi Bahaya Gempa Indonesia untuk Perencanaan dan Evaluasi Infrastruktur Tahan Gempa*, Pusat Studi Gempa Nasional, 2022.
14. *DEEPSOIL V.7,* University of Illinois, 2020.
15. *PEER Ground Motion Database*, Pacific Earthquake Engineering Research Center, 2022, retrieved from http://ngawest2.berkeley.edu
16. FEMA P-2091, *A Practical Guide to Soil-Structure Interaction*, Applied Technology Council, 2020.
17. SNI 1727:2020, *Beban Minimum untuk Perancangan Bangunan Gedung dan Struktur Lain,* Badan Standardisasi Nasional, 2020.
18. SNI-03-1726-2019, *Tata Cara Perencanaan Ketahanan Gempa untuk Struktur Bangunan Gedung dan Non Gedung*, Badan Standardisasi Nasional, 2019.